ANALYTICAL SOLUTIONS OF THE SCATTERING OF PLANE WAVES BY LOCAL SITES WITH SATURATED SOIL

Weihua Li[1] and Chenggang Zhao[2]

1 Doctor, Dept. of civil Engineering , Beijing Jiaotong University, Beijing. China
2 Professor, Dept. of civil Engineering, Beijing Jiaotong University, Beijing. China
Email: whli@bjtu.edu.cn

ABSTRACT:
The ground amplification effects caused by irregular surface topography and geological conditions have been the focus of research by both seismologists and earthquake engineers for the last three decades. Many methods have been developed. However, only few analytical solutions are available so far, and the majority of the solutions for the wave propagation are supposed in the single-phase elastic medium. In this paper, the earthquake ground motions of local irregular sites with saturated soil were investigated by analytical solutions, and a series of results were obtained. Firstly, on the basis of Biot dynamic theory, an analytical method for scattering of plane waves by saturated soil was developed using Fourier-Bessel series expansion technique. Using this method, a series of analytical solutions for scattering of plane waves by saturated soil local irregular site can be got. Secondly, on the base of the analytical solutions mentioned above, the numerical results were given to illustrate that the ground motions of the saturated soil local irregular site not only depend on the angle of incidence, the dimensionless frequency of the incident waves, but also depend on the saturation and porosity of the soil deposits, the stiffness and Poisson's ratio of the solid-skeleton, and the boundary conditions. At the same time, the soft saturated soil site can be simulated by elastic one-phase solid model or by fluid-saturated porous media model, but the results of the ground motion by the two models were great different.
KEYWORDS: Fluid saturated porous medium, Complex local site, Scattering of seismic waves, Analytical solution

1. INTRODUTION

In many areas of seismological research, the ground amplification effects caused by local irregular sites can be an important factor [1]. Therefore, a detailed understanding of these effects is of obvious value to earth- quake engineering and seismology, and such effects have been recognized widely as an important factor and extensive theoretical and experimental works have been carried out on the subject in the last 3 decades. Various theoretical analysis methods have been developed to study the effects of irregular surface topography and geological conditions on the ground amplification. In general, these methods can be classified as analytical methods and numerical methods. It is believe that the earliest method to be used in treatment of the wave propagation problems is due to analytical method. This kind of methods includes separated variable method, integral-transformation method, and wave function expansion method, etc. and is applied mainly to the problems with linear, isotropic and homogeneous materials and simple geometries. Because modeling the seismic wave scattering by local sites involves great complexities, very few analytical solutions are available so far, which are: scattering of plane SH wave by semi-cylindrical and semi-elliptical canyon and alluvial valley[2-5]; scattering of plane P, SV, SH, and Rayleigh waves by circular- cylindrical canyon and alluvial valley[6-9]; scattering of plane P, SV, and SH waves by circular-arc layered alluvial valleys[10][11]; scattering of plane P, SV and SH wave by hemispherical canyon and alluvial valley[12][13]. As a result of the limitation of analysis methods, the role of numerical methods is increasingly concerned in studying the problems of wave propagations in complex medium, and various numerical methods, such as the finite differential method, the finite element method, and the boundary element method, etc. have been developed. More detail review of these studies can be found in literature by Li.[14]
In a word, the methods used to study the ground motion amplification effects caused by local sites have got great development. But, it is worth paying attention to that all above-mentioned studies are supposed in the single-phase elastic medium. In fact, geomaterials are often present in the form of porous solid saturated by fluid in nature. Therefore, the study of dynamic response of a fluid-saturated porous medium is of considerable interest to applications in geotechnical and earthquake engineering [15]. Biot [16] developed the propagation

theory of elastic waves in fluid saturated porous media. But up to date, there is very few analytical solutions available for the scattering of plane waves by irregular surface in saturated porous media based on the Biot dynamic theory so far. [17][18] Complexities of wave propagation in saturated porous media pose additional challenge for the modeling of scattering problems. Therefore, there is a need to develop a systematic approach which leads to the solution of scattering problems with saturated porous media.
The purpose of this paper is to illustrate the methods for solution of the problem about scattering of plane waves by saturated soil local site and the effects of surface and subsurface irregularities on ground motion amplification. The method of analysis used is wave function expansion method. Firstly, the wave function expansions of elastic waves in fluid-saturated porous medium are deduced on the basis of Biot dynamic theory. Based on this method and combined with the boundary conditions of each problem, a series of analytical solutions for scattering of plane P and SV waves by several typical sites with saturated soil can be developed , which include: (1) cylindrical canyons in saturated porous medium; (2) alluvial valleys with saturated soil deposits; (3) circular-arc layered valleys consisting of the interaction between water and saturated soil deposits; (4) cylindrical cavity in a fluid-saturated porous media half space. Secondly, on the base of the analytical solutions, the influence factors of the earthquake ground motions are studied. At the same time, the soft saturated soil site can be simulated by elastic one-phase solid model or by fluid-saturated porous media model, but the results of the ground motion by the two models were great different.

2. THEROY OF WAVE PROPOGATION AND WAVE FUNCTION EXPANSIONS IN FLUID-SATURATED POROUS MEDIUM

2.1 Wave equations

The dynamic equations for saturated porous media with non-viscous fluid proposed by Biot [16] are

$$N\nabla^2 u+\nabla[(A+N)e+Q\varepsilon]=\left(\rho_{11}\frac{\partial^2 u}{\partial t^2}+\rho_{12}\frac{\partial^2 U}{\partial t^2}\right)+b\left(\frac{\partial u}{\partial t}-\frac{\partial U}{\partial t}\right),\quad \nabla[Qe+R\varepsilon]=\left(\rho_{12}\frac{\partial^2 u}{\partial t^2}+\rho_{22}\frac{\partial^2 U}{\partial t^2}\right)-b\left(\frac{\partial u}{\partial t}-\frac{\partial U}{\partial t}\right) \quad (2.1)$$

where u and U are the displacements of solid phase and liquid phase respectively; $e=\nabla\cdot u$, $\varepsilon=\nabla\cdot U$, $\rho_{11}=\rho_1+\rho_a$, $\rho_{22}=\rho_2+\rho_a$, $\rho_{12}=-\rho_a$, $\rho_1=(1-n)\rho_s$, $\rho_2=n\rho_f$, where ρ_s, ρ_f, and ρ_a are the density of solid mass, liquid mass, and coupled-mass between solid phase and liquid phase; b is the dissipative coefficient, $b=\zeta n^2/k$, in which ζ is the absolute viscosity, n is porosity, and k is permeability; and N, A, R and Q are elastic modules which are defined as: $R=nK_f$, $Q=(1-n)K_f$, $N=\mu$, $A=\lambda+Q^2/R$, where λ and μ are the Lame constants of the solid skeleton in the saturated porous media, and K_f is the bulk modulus of pore water. In this paper, a non-dissipative case (ζ=0) is considered. The constitutive equation for a porous elastic solid containing compressible fluid can be expressed as

$$\tau_{ij}=2N\varepsilon_{ij}+\delta_{ij}(Ae+Q\varepsilon),\qquad \sigma=Qe+R\varepsilon \quad (2.2)$$

where τ_{ij} is the stress in the solid skeleton, σ is the fluid pore pressure, and $\delta_{ij}=\begin{cases}1, & i=j\\ 0, & i\neq j\end{cases}$, $\varepsilon_{ij}=\dfrac{u_{i,j}+u_{j,i}}{2}$.

2.2 Solutions of wave equations

To solve the governing Eqn. (1), the Helmoltz resolution [19] is applied as follows

$$\boldsymbol{u}=\text{grad}\,\phi+\text{curl}\,\psi\,;\ \boldsymbol{U}=\text{grad}\,\Phi+\text{curl}\,\Psi \quad (2.3)$$

where the potential functions □ and ψ are associated with the solid phase of the bulk material, while the potential functions Φ and Ψ are associated with the pore fluid. If the wave potentials have harmonic time variations, the potentials can be expressed as

$$\phi=\phi(x,y,z)e^{-i\omega t},\quad \Phi=\Phi(x,y,z)e^{-i\omega t},\quad \psi=\psi(x,y,z)e^{-i\omega t},\quad \Psi=\Psi(x,y,z)e^{-i\omega t} \quad (2.4)$$

Substituting Eqns. (2.3) and (2.4) into Eqn. (2.1), the following two equations with respect to P-wave and S-wave potentials of the solid phase are obtained

$$(\nabla^2 + k_{a,j}^2)\phi_j = 0 \quad (j=1, 2);\quad (\nabla^2 + k_\beta^2)\psi = 0 \tag{2.5}$$

where $k_{a,j} = \dfrac{\omega}{V_{a,j}}$ (j=1,2) and $k_\beta = \dfrac{\omega}{V_\beta}$ are the P and S wave-numbers, and $V_{a,j} = \sqrt{\dfrac{2B}{C \mp (C^2 - 4BD)^{1/2}}}$ (j =1,2) and $V_\beta = \sqrt{\dfrac{N\rho_{22}}{D}}$ are the P and S wave velocities respectively with $B = PR - Q^2$, $C = \rho_{11}R + \rho_{22}P - 2\rho_{12}Q$, $D = \rho_{11}\rho_{22} - \rho_{12}^2$.

From Eqn. (2.5), it is seen that there are two dilatational waves (referred to as P_I wave and P_{II} wave, respectively) and one rotational wave (S wave). The general solution P-waves for the solid phase is

$$\phi = \phi_1 + \phi_2 \tag{2.6}$$

Substituting Eqns. (2.3) and (2.4) into Eqn. (2.1), the wave potentials for the fluid component also can been obtained

$$\Phi = \Phi_1 + \Phi_2 = \eta_I\phi_1 + \eta_{II}\phi_2 \qquad \Psi = \eta_3\psi \tag{2.7}$$

where $\eta_j = \dfrac{B/V_{a,j}^2 - \rho_{11}R + \rho_{12}Q}{\rho_{12}R - \rho_{22}Q}$ (j=1, 2) $\eta_3 = -\dfrac{\rho_{12}}{\rho_{22}}$.

2.3 Wave function expansions in cylindrical coordinates

The models presented in this paper are all two-dimensional plan strain problems, so in a cylindrical coordinate system Eqn. (2.6) can be expressed as:

$$\phi = \phi(r,\theta)e^{-i\omega t},\quad \Phi = \Phi(r,\theta)e^{-i\omega t},\quad \psi = \psi(r,\theta)e^{-i\omega t},\quad \Psi = \Psi(r,\theta)e^{-i\omega t} \tag{2.8}$$

Taking the wave function of P_I waves for example, wave function expansions in cylindrical coordinates will be introduced as bellow.

In cylindrical coordinates for plan strain problems, the fist equation of Eqn. (2.5) with j=1 can be expressed as

$$\frac{1}{r}\frac{\partial}{\partial r}\left(r\frac{\partial \phi_1}{\partial r}\right) + \frac{1}{r^2}\frac{\partial^2\phi_1}{\partial\theta^2} + k_{a,1}^2\phi_1 = 0 \tag{2.9}$$

By using the method of separation of variables with $\phi_1(r,\theta) = R(r)\Theta(\theta)$, Eq. (2.9) separates into

$$r^2R'' + rR' + (k_{a,1}^2r^2 - v^2)R = 0,\quad \Theta'' + v^2\Theta = 0 \tag{2.10}$$

where v is the separation constant. For most problems of interest, □1 must be single valued, so $\Theta(\theta + 2\pi) = \Theta(\theta)$, which requires $v=n$, where n in an integer. The first equation of Eqn. (2.10) then becomes

$$r^2R'' + rR' + (k_{a,1}^2r^2 - n^2)R = 0 \tag{2.11}$$

with solution that can be expressed linear combination of either Bessel functions of the fist and second kind, $J_n(k_{a,1}r)$ and $Y_n(k_{a,1}r)$, or Hankel functions of the fist and second kind, $H_n^{(1)}(k_{a,1}r)$ and $H_n^{(2)}(k_{a,1}r)$. That is

$$R(r) = A_n J_n(k_{a,1}r) + B_n Y_n(k_{a,1}r) \quad \text{or} \quad R(r) = \widetilde{A}_n H_n^{(1)}(k_{a,1}r) + \widetilde{B}_n H_n^{(2)}(k_{a,1}r) \tag{2.12}$$

where A_n, B_n, $\widetilde{A}_n$, and $\widetilde{B}_n$ are random constants. The choice of the radial functions, i.e., $J_n(k_{a,1}r)$ and $Y_n(k_{a,1}r)$ or $H_n^{(1)}(k_{a,1}r)$ and $H_n^{(2)}(k_{a,1}r)$, is dependent upon the physics of the problem.

The general solution of the second equation of Eqn. (2.10) is

$$\Theta(\theta) = C_n\cos n\theta + D_n\sin n\theta \tag{2.13}$$

where C_n and D_n are random constants. Then the solution of the wave function □1 can be expressed as

$$\phi_1(r,\theta) = \sum_{n=0}^{\infty}\left[A_n J_n(k_{a,1}r) + B_n Y_n(k_{a,1}r)\right]\left(C_n\cos n\theta + D_n\sin n\theta\right) \quad \text{or} \quad \phi_1(r,\theta) = \sum_{n=0}^{\infty}\left[\widetilde{A}_n H_n^{(1)}(k_{a,1}r) + \widetilde{B}_n H_n^{(2)}(k_{a,1}r)\right]\left(C_n\cos n\theta + D_n\sin n\theta\right) \tag{2.14}$$

with the time factor $\exp(i\omega t)$ being omitted. Therefore, the wave functions of steady-state waves can be expressed the combination of $J_n(k_{a,1}r)$ and $Y_n(k_{a,1}r)$ or $H_n^{(1)}(k_{a,1}r)$ and $H_n^{(2)}(k_{a,1}r)$ with $\cos n\theta$ and $\sin n\theta$. This constitutes the foundation of wave function expansion method.

3. THE BOUNDARY VALUE PROBLEMS CONSIDERED IN THIS PAPER

It is seen that the method developed above can provide the foundation for the further analysis of the scattering and diffraction of P, SV and Rayleigh waves by the alluvial valleys and other irregular topography conditions in a half space of saturated porous media. This paper only focuses on the researches of scattering of plane P and SV waves by several typical sites with saturated soil as follows.

3.1 Cylindrical canyons in saturated porous medium (problem 1)

The two-dimensional model of problem 1 used in this paper is shown in Fig. 1. It represents a half space (y>0) from which a vector of a circle of radius a_1 and centered at o_1 is removed to form a canyon. The width of the circular sector at the surface of the half space is $2a$ and its depth is h. The half space is assumed to be saturated porous material.
In a wave propagation problem, it is important to employ appropriate boundary conditions. Deresiewicz, et.al.[19][20] proposed the boundary conditions for two different fluid-saturated porous media in contact. One is open (pervious)-boundary, and the other is sealed (impervious)-boundary. So the boundary conditions on the surface of the canyon can be stated as: for pervious boundary conditions

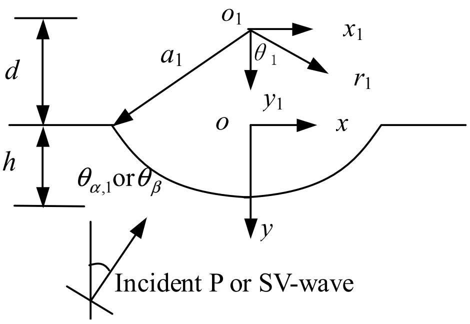

Fig.1 The model of problem 1

$$\tau^v_{yy} = \tau^v_{xy} = 0\,,\quad \sigma^v = 0 \quad \text{at} \quad y=0 \quad \text{and} \quad \tau^v_{r\theta} = \tau^v_{rr} = 0\,,\quad \sigma^v = 0 \quad \text{at} \quad r_1=a_1 \tag{3.1a}$$

or for impervious boundary conditions

$$\tau^v_{yy} + \sigma^v = \tau^v_{xy} = 0\,,\quad u^v_y - U^v_y = 0 \quad \text{at} \quad y=0 \text{ and } \tau^v_{r\theta} = \tau^v_{rr} + \sigma^v = 0\,,\quad u^v_r - U^v_r = 0 \quad \text{at} \quad r_1=a_1 \tag{3.1b}$$

3.2 Circular-arc alluvial valleys with saturated soil deposits (problem 2)

The two-dimensional model of problem 2 to be analyzed is shown in Fig. 2. The circular-arc alluvial valley with saturated soil deposits is embedded in an infinite half-space (y>0). The valley is bounded by a flat ground surface, and the shape of the circular-arc is characterized by its center, o_1, radius, a_1, depth, h, and width, $2a$ as shown in Fig. 2. The half- space is assumed as a single-phase, elastic, isotropic, and homogenous solid, with its properties characterized by Lame constants, λ and μ , and mass density, ρ . The soil deposit is modeled as a saturated porous medium.
The boundary conditions of this problem include zero-stress at the free ground surface, and the continuity conditions at the interface [20] [21] between the valley and half space. These can be expressed as

$$\tau^v_{yy} = \tau^v_{yx} = \sigma^v = 0 \quad \tau^s_{yy} = \tau^s_{yx} = 0 \quad \text{at} \quad y = 0 \tag{3.2}$$

$$u^v_r = u^s_r \quad u^v_\theta = u^s_\theta \quad \tau^v_{rr} + \sigma^v = \tau^s_{rr} \quad \tau^s_{r\theta} = \tau^v_{r\theta} \quad \text{at}\ r_1 = a_1 \tag{3.3}$$

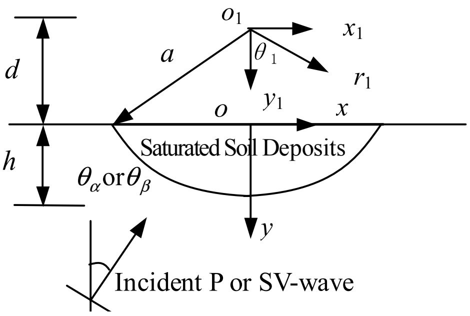

Fig.2 The model of problem 2

It is also necessary to add a hydraulic condition at the interface:

$$u^v_r - U^v_r = 0 \quad \text{at}\ r_1 = a_1 \text{ (for impermeable interface) or } \sigma^v = 0 \quad \text{at} \quad r_1 = a_1 \text{ (for permeable interface)} \tag{3.4}$$

where, the superscripts, s and v, indicate the half space and valley, respectively.

3.3 Circular-arc layered valley with saturated soil deposits and water (problem 3)

A cross-section of the two-dimensional model to be analyzed is shown in Fig. 3. The circular-arc layered valley with saturated soil deposits and water is embedded in an infinite half-space (y>0). The valley is bounded by a flat ground surface, and the shape of the circular-arc is characterized by its center, o_1, radius, b_2, depth, h_2, and width, $2a_2$. The interface between water and saturated soil deposits is also circular-arc with center, o_1, radius, b_1, depth, h_1, and width, $2a_1$ as shown in Fig. 3. The half- space is assumed as a single-phase, elastic, isotropic, and homogenous solid, with its properties characterized by physical parameters, Lame constants, λ and μ , and mass density, ρ . The soil deposit is modeled as a saturated porous medium, and the water in the valleys is simulated by non-viscous perfect fluid. The wave equations of the perfect fluid was expressed by Wang [22] as follows

$$\rho_f \frac{\partial^2 u_f}{\partial t^2} = K_f \nabla\nabla \cdot u_f \tag{3.5}$$

where ρ_f, K_f , and u_f are the density, incompressible coefficient, and displacement of the fluid respectively. From Eqn. (3.5), it is seen that only P-waves exist in the non-viscous perfect fluid with the velocity of $\sqrt{K_f/\rho_f}$.

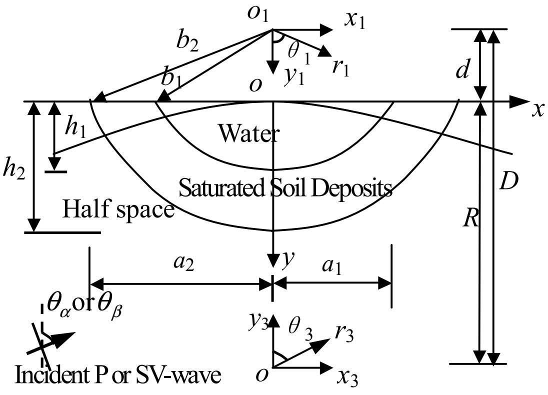

Fig.3 The model of problem 3

The boundary conditions of this problem include zero-stress at the free ground surface within the valley and the half space out of the valley, and the continuity conditions at the interface between the valley and half space, and between the saturated soil deposits and water. Assuming the ground surface within the valley to be pervious, the zero-stress boundary conditions can be expressed as

$$\tau^s_{yy}=\tau^s_{yx}=0 \ , \quad \tau^v_{yy}=\tau^v_{yx}=\sigma^v=0 \ , \quad \tau^w_{yy}=0 \quad \text{at } y=0 \tag{3.6}$$

where, the superscripts, s ,v, and w, indicate the half space, valley and water, respectively.

If the interface between the valley and half space is permeable, the continuity conditions at the interface can be expressed as:

$$u^v_r=u^s_r \ , \quad u^v_\theta=u^s_\theta \ , \quad \tau^v_{rr}=\tau^s_{rr} \ , \quad \sigma^v=0 \ , \quad \tau^v_{r\theta}=\tau^s_{r\theta} \qquad \text{at } r_1=b_2 \tag{3.7}$$

The continuity conditions at the interface between the saturated soil deposits and water are

$$(1-n)u^v_r+nU^v_r=u^w_r \ , \quad \tau^v_{r\theta}=0 \ , \quad \tau^v_{rr}+\sigma^V=\tau^w_{rr} \ , \quad \sigma^v=-n\tau^w_{rr} \quad \text{at } r_1=b_1 \tag{3.8}$$

3.4 Cylindrical cavity in a fluid-saturated porous medium half space (problem 4)

Fig.4 shows the model of problem 4. The half-space is made of a fluid-saturated porous medium defined by the x-y coordinate system for $y>0$, and is uniform expect for the circular cylindrical section of radius a that is removed to form an unlined cavity. The cylinder is centered at a depth h below the half-space surface.

The boundary conditions of this problem are the stress-free boundary conditions at the half space and cavity surface. It is obvious that there are two kinds of boundary conditions as problem 1, one is pervious boundary conditions which can be expressed as:

$$\tau^v_{yy}=\tau^v_{xy}=0 \ , \quad \sigma^v=0 \quad \text{at} \quad y=0 \quad \text{and} \quad \tau^v_{r\theta}=\tau^v_{rr}=0 \ , \sigma^v=0 \quad \text{at} \quad r_1=a \tag{3.9a}$$

and the other is impervious boundary conditions:

$$\tau^v_{yy}+\sigma^v=\tau^v_{xy}=0 \ , \quad u^v_y-U^v_y=0 \quad \text{at} \quad y=0 \text{ and } \quad \tau^v_{r\theta}=\tau^v_{rr}+\sigma^v=0 \ , \quad u^v_r-U^v_r=0 \quad \text{at} \quad r_1=a \tag{3.9b}$$

In the four questions, assuming the excitation in the half space to be a sinusoidal plane P or SV wave with circular frequency ω and incident angle of θ_α (for P wave) or θ_β (for SV wave). The displacement and propagation vector are situated in the x-y plane.

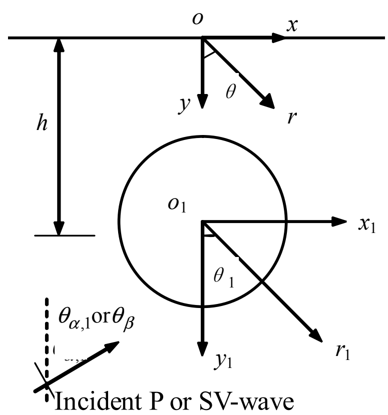

Fig.4 The model of problem4

4. THE SOLUTIONS

In this section, the solution of problem 3 for incident SV-wave will be taken for example to illustrate the methods for solution of scattering of plane waves by above mentioned four typical sites with saturated soil. The details of the other three problem solutions can be found in Ref. [15].

4.1 Wave field analysis

4.1.1 Free wave field

By omitting the time factor exp(-iωt), the potential function of the incident SV wave, in the (x,y) coordinate system, can be expressed as

$$\psi_s^{(i)} = \exp[ik_{s2}(x\sin\theta_\beta - y\cos\theta_\beta)] \tag{4.1}$$

in which, k_{s2} is the longitudinal wave number. If there is no circular valley, the incident SV wave reflected from the half space will generate a reflected P as well as a SV wave to satisfy the stress-free boundary conditions. The reflected SV is plane wave, whereas the P wave may be either: (1) plane body waves, if incident angle is below the critical angle θ_{cr} ($\theta_\beta<\theta_{cr}$), or (2) surface waves if $\theta_{cr}>\theta_\beta$. The critical angle is θ_{cr}=sin(k_{s1}/k_{s2}).

Case 1. Incident at or below critical angle ($\theta_\beta<\theta_{cr}$). The reflected P wave and SV wave potential functions are

$$\phi_s^{(r)} = A_{s1}\exp[ik_{s1}(x\sin\theta_\alpha + y\cos\theta_\alpha)]\,,\,\psi_s^{(r)} = A_{s2}\exp[ik_{s2}(x\sin\theta_\beta + y\cos\theta_\beta)] \tag{4.2}$$

where, k_{s1} is the wave number and θ_α is the reflected angle of the P wave. The relationship between θ_α and θ_β is $k_{s1}\sin\theta_\alpha = k_{s2}\sin\theta_\beta$. A_{s1} and A_{s2} are the reflection coefficients. Eqns. (4.1) and (4.2) also can be expanded in terms of Fourier-Bessel series in the cylindrical coordinates (r_1, θ_1) as incident plane P-waves

$$\phi_s^{(r)}(r_1,\theta_1) = \sum_{n=0}^{\infty} J_n(k_{s1}r_1)(A_{0n}\cos n\theta_1 + B_{0n}\sin n\theta_1), \psi_s^{(i+r)}(r_1,\theta_1) = \sum_{n=0}^{\infty} J_n(k_{s2}r_1)(C_{0n}\sin n\theta_1 + D_{0n}\cos n\theta_1) \tag{4.3}$$

where

$$\begin{Bmatrix} A_{0n} \\ B_{0n} \end{Bmatrix} = \varepsilon_n \begin{Bmatrix} \cos n\theta_\alpha \\ \sin n\theta_\alpha \end{Bmatrix} (i)^n A_{s1}\exp(-idk_{s1}\cos\theta_\alpha)]\,;\, \begin{Bmatrix} C_{0n} \\ D_{0n} \end{Bmatrix} = \varepsilon_n (i)^n \begin{Bmatrix} \sin n\theta_\alpha \\ \cos n\theta_\alpha \end{Bmatrix} \begin{bmatrix} \mp(-1)^n \exp(idk_{s2}\cos\theta_\beta) \\ + A_{s2}\exp(-idk_{s2}\cos\theta_\beta) \end{bmatrix} \tag{4.4}$$

Case 2. Incidence beyond critical angle($\theta_\beta>\theta_{cr}$). In this case, the reflected angle of the P wave, θ_α, becomes complex, and the reflect P-wave is an inhomogeneous (surface) wave. Then in the cylindrical coordinates (r_1, θ_1) □$_s^{(r)}$ can be written as

$$\phi_s^{(r)}(r_1,\theta_1) = A_{s1}\exp(\gamma d)\exp[-\gamma\ \ r_1\cos\theta_1 + ikr_1\sin\theta_1] \tag{4.5}$$

Where γ= -$ik_1\cos\theta_\alpha$ is a real value quantity and k=$k_{s1}\sin\theta_\alpha$=$k_{s2}\sin\theta_\beta$ is the horizontal wave number of the incident and of the reflected waves. Now an expansion of the potential function in terms of Fourier–Bessel series as above in the full space would not be appropriate, since it is also exponentially increasing in the negative y-axis, and hence unbounded. Lee and Cao [8] in their paper on scattering of plane SV-waves from shallow circular canyons expanded the potential function of the reflected P wave along the surface of the canyon in finite Fourier series of θ_1 with period 2π. Because the function that they approximated had jumps at θ_1=θ_0 and θ_1=-θ_0, the finite Fourier series and its derivatives could oscillate significantly about the exact function in the neighborhood of the boundary points. To overcome this disadvantage, in this paper a modified version of the method of Ref.[8] is used. The displacements and the stresses at r_1=b_2 are fist calculated directly by differentiating the expression for □$_s^{(r)}$(r_1, θ_1), and then those are expanded in finite Fourier series of θ_1. If u_r^{s,ϕ_s}, u_θ^{s,ϕ_s}, τ_{rr}^{s,ϕ_s} and $\tau_{r\theta}^{s,\phi_s}$ are the displacements and the stresses induced by □$_s^{(r)}$(r_1, θ_1)only, then

$$\left.\begin{aligned} u_r^{s,\phi_s}(a_1,\theta_1) &= \left.\frac{\partial\phi_s^{(r)}}{\partial r_1}\right|_{r=a_1} = ik_{s1}\cos(\theta_1-\theta_\alpha)\phi_s^{(r)}(a_1,\theta_1)\,,\, u_\theta^{s,\phi_s}(a_1,\theta_1) = \left.\frac{1}{r_1}\frac{\partial\phi_s^{(r)}}{\partial\theta_1}\right|_{r_1=a_1} = -ik_{s1}\sin(\theta_1-\theta_\alpha)\phi_s^{(r)}(a_1,\theta_1) \\ \tau_{rr}^{s,\phi_s}(a_1,\theta_1) &= \left[\lambda\nabla^2\phi_s^{(r)} + 2\mu\left(\frac{\partial^2\phi_s^{(r)}}{\partial r_1^{\,2}}\right)\right]_{r_1=a_1} = -\left[\lambda k_{s1}^2 + 2\mu k_{s1}^2\cos^2(\theta_1-\theta_\alpha)\right]\phi_s^{(r)}(a_1,\theta_1) \\ \tau_{r\theta}^{s,\phi_s}(a_1,\theta_1) &= 2\mu\left(\frac{1}{a_1}\frac{\partial^2\phi_s^{(r)}}{\partial r_1\partial\theta_1} - \frac{1}{a_1^2}\frac{\partial\phi_s^{(r)}}{\partial\theta_1}\right)_{r_1=a_1} = 2\mu k_{s1}^2\sin(\theta_1-\theta_\alpha)\cos(\theta_1-\theta_\alpha)\phi_s^{(r)}(a_1,\theta_1) \end{aligned}\right\} \tag{4.6}$$

And the expansions of u_r^{s,ϕ_s}, u_θ^{s,ϕ_s}, τ_{rr}^{s,ϕ_s} and $\tau_{r\theta}^{s,\phi_s}$ in finite Fourier series can be expressed:

$$u_r^{s*}(a_1,\theta_1) = \sum_{n=0}^{N}\left[A_{0n}^{u_r}\cos n\theta_1 + B_{0n}^{u_r}\sin n\theta_1\right],\quad \tau_{rr}^{s*}(a_1,\theta_1) = \sum_{n=0}^{N}\left[A_{0n}^{\tau_r}\cos n\theta_1 + B_{0n}^{\tau_r}\sin n\theta_1\right],\quad \tau_{r\theta}^{s*}(a_1,\theta_1) = \sum_{n=0}^{N}\left[A_{0n}^{\tau_\theta}\sin n\theta_1 + B_{0n}^{\tau_\theta}\cos n\theta_1\right] \tag{4.7}$$

The coefficients $\{A_{0n}^{u_r}\}_{n=0}^{N}$, $\{B_{0n}^{u_r}\}_{n=0}^{N}$, $\{A_{0n}^{u_\theta}\}_{n=0}^{N}$, $\{B_{0n}^{u_\theta}\}_{n=0}^{N}$, $\{A_{0n}^{\tau_r}\}_{n=0}^{N}$, $\{B_{0n}^{\tau_r}\}_{n=0}^{N}$, $\{A_{0n}^{\tau_\theta}\}_{n=0}^{N}$, $\{B_{0n}^{\tau_\theta}\}_{n=0}^{N}$ can be calculated as in Ref.[7]. In the following discussions, the above expansions of u_r^{s,ϕ_s}, u_θ^{s,ϕ_s}, τ_{rr}^{s,ϕ_s} and $\tau_{r\theta}^{s,\phi_s}$ induced by □$_s^{(r)}(r_1,\ \theta_1)$ can be introduced into the boundary conditions directly.

4.1.2 Scattered wave field

For convenient to introduce the boundary conditions, the large circle assumption introduced by Cao and Lee [13] is applied in this work. That is the half space boundary is approximated as a nearly flat circular boundary centered at o_3 with a radius R (Fig.3). It is now obvious that when the radius of the large circle approaches infinity this model approaches that of the circular-arc alluvial valley in the half space.

Scattered waves in the half space

In the half space, because of the presence of both the plane free boundary and the circular-arc layered valley, the incident SV wave and the reflected P and SV waves from the ground surface will be scattered and diffracted around the valley in the half space, and the scattered cylindrical waves from the valley will be reflected back into the half space from the plane free surface. These two sets of waves can be characterized by the following potential functions

$$\begin{cases} \phi_{s2}(r_1,\theta_1)=\sum_{n=0}^{\infty}H_n^{(1)}(k_1r_1)(A_{s2,n}^{(1)}\cos n\theta_1+B_{s2,n}^{(1)}\sin n\theta_1) \\ \psi_{s2}(r_1,\theta_1)=\sum_{n=0}^{\infty}H_n^{(1)}(k_2r_1)(C_{s2,n}^{(1)}\sin n\theta_1+D_{s2,n}^{(1)}\cos n\theta_1) \end{cases} \tag{4.8}$$

$$\begin{cases} \phi_{s3}(r_3,\theta_3)=\sum_{m=0}^{\infty}J_m(k_1r_3)(A_{s3,m}^{(3)}\cos m\theta_3+B_{s3,m}^{(3)}\sin m\theta_3) \\ \psi_{s3}(r_3,\theta_3)=\sum_{m=0}^{\infty}J_m(k_2r_3)(C_{s3,m}^{(3)}\sin m\theta_3+D_{s3,m}^{(3)}\cos m\theta_3) \end{cases} \tag{4.9}$$

Scattered waves in the saturated soil deposits

In the saturated soil deposits of the valley, there are three sets of newly-generated waves because of the presence of stress-free ground surface, the interface between the half space and the circular-arc alluvial valley and the interface between the saturated soil deposits and water. According to Biot's dynamic theory, there are three types of waves in each set, including two types of compressional waves, i.e. P_{I} and P_{II} waves, and one shear wave, i.e. SV wave. Their potential functions can be expressed as follows

$$\begin{cases} \phi_{1,v1}(r_1,\theta_1)=\sum_{n=0}^{\infty}J_n(k_{\alpha,1}r_1)(A_{v1,n}^{(1)}\cos n\theta_1+B_{v1,n}^{(1)}\sin n\theta_1) \\ \phi_{2,v1}(r_1,\theta_1)=\sum_{n=0}^{\infty}J_n(k_{\alpha,2}r_1)(C_{v1,n}^{(1)}\cos n\theta_1+D_{v1,n}^{(1)}\sin n\theta_1) \\ \psi_{v1}(r_1,\theta_1)=\sum_{n=0}^{\infty}J_n(k_\beta r_1)(E_{v1,n}^{(1)}\sin n\theta_1+F_{v1,n}^{(1)}\cos n\theta_1) \end{cases} \tag{4.10}$$

$$\begin{cases} \phi_{1,v2}(r_1,\theta_1)=\sum_{n=0}^{\infty}H_n^{(1)}(k_{\alpha,1}r_1)(A_{v2,n}^{(1)}\cos n\theta_1+B_{v2,n}^{(1)}\sin n\theta_1) \\ \phi_{2,v2}(r_1,\theta_1)=\sum_{n=0}^{\infty}H_n^{(1)}(k_{\alpha,2}r_1)(C_{v2,n}^{(1)}\cos n\theta_1+D_{v2,n}^{(1)}\sin n\theta_1) \\ \psi_{v2}(r_1,\theta_1)=\sum_{n=0}^{\infty}H_n^{(1)}(k_\beta r_1)(E_{v2,n}^{(1)}\sin n\theta_1+F_{v2,n}^{(1)}\cos n\theta_1) \end{cases} \tag{4.11}$$

$$\begin{cases} \phi_{1,v3}(r_3,\theta_3)=\sum_{m=0}^{\infty}J_m(k_{\alpha,1}r_3)(A_{v3,m}^{(3)}\cos m\theta_3+B_{v3,m}^{(3)}\sin m\theta_3) \\ \phi_{2,v3}(r_3,\theta_3)=\sum_{m=0}^{\infty}J_m(k_{\alpha,2}r_3)(C_{v3,m}^{(3)}\cos m\theta_3+D_{v3,m}^{(3)}\sin m\theta_3) \\ \psi_{v3}(r_3,\theta_3)=\sum_{m=0}^{\infty}J_m(k_\beta r_3)(E_{v3,m}^{(3)}\sin m\theta_3+F_{v3,m}^{(3)}\cos m\theta_3) \end{cases} \tag{4.12}$$

where $k_{a,1}$, $k_{a,2}$and k_β are wave numbers of P□, P□ and SV waves respectively which were defined in section 2.2.

Scattered waves in the water

In the layer of fluid medium, there are two sets of newly-generated waves because of the presence of stress-free ground surface, the interface between the saturated soil deposits and water. Their potential functions can be expressed as follows

$$\phi_{w2}(r_1,\theta_1)=\sum_{n=0}^{\infty}J_n(k_wr_1)(A_{w2,n}^{(1)}\cos n\theta_1+B_{w2,n}^{(1)}\sin n\theta_1) \tag{4.13}$$

$$\phi_{w3}(r_3,\theta_3)=\sum_{m=0}^{\infty}J_m(k_wr_3)(A_{w3,m}^{(3)}\cos m\theta_3+B_{w3,m}^{(3)}\sin m\theta_3) \tag{4.14}$$

where k_w is the wave number of P-wave in the fluid medium。

In Eqns. (4.8) - (4.14) $\{A_{w2,n}^{(1)}\quad B_{w2,n}^{(1)}\}$, $\{A_{w3,m}^{(3)}\quad B_{w3,m}^{(3)}\}$, $\{A_{s2,n}^{(1)}\quad B_{s2,n}^{(1)}\quad C_{s2,n}^{(1)}\quad D_{s2,n}^{(1)}\}$, $\{A_{s3,m}^{(3)}\quad B_{s3,m}^{(3)}\quad C_{s3,m}^{(3)}\quad D_{s3,m}^{(3)}\}$,

$\{A_{v1,n}^{(1)}\ B_{v1,n}^{(1)}\ C_{v1,n}^{(1)}\ D_{v1,n}^{(1)}\ E_{v1,n}^{(1)}\ F_{v1,n}^{(1)}\}$, $\{A_{v2,n}^{(1)}\ B_{v2,n}^{(1)}\ C_{v2,n}^{(1)}\ D_{v2,n}^{(1)}\ E_{v2,n}^{(1)}\ F_{v2,n}^{(1)}\}$, $\{A_{v3,m}^{(3)}\ B_{v3,m}^{(3)}\ C_{v3,m}^{(3)}\ D_{v3,m}^{(3)}\ E_{v3,m}^{(3)}\ F_{v3,m}^{(3)}\}$, are the undetermined coefficients.

The above mentioned potential functions are expressed in different cylindrical coordinates. To be convenient to solve the problem, it is need to perform coordinate transformations. According to the Graf's addition formula[23].

$$C_n(kr_1)\begin{Bmatrix}\cos n\theta_1\\ \sin n\theta_1\end{Bmatrix}=\sum_{m=-\infty}^{m=+\infty}C_{m+n}(kD)J_m(kr_3)\begin{Bmatrix}\cos m\theta_3\\ \sin m\theta_3\end{Bmatrix}(r_3<D)\,,C_m(kr_3)\begin{Bmatrix}\cos m\theta_3\\ \sin m\theta_3\end{Bmatrix}=\sum_{n=-\infty}^{n=+\infty}C_{n+m}(kD)J_n(kr_1)\begin{Bmatrix}\cos n\theta_1\\ \sin n\theta_1\end{Bmatrix}(r_1<D)\quad(4.15)$$

where $C_n(\bullet)$ represents $J_n(\bullet)$ or $H^{(1)}{}_n(\bullet)$, and D is the distance between o_1 and o_3. The wave potential functions Eqns. (4.8) - (4.14) can be expressed using the other corresponding cylindrical coordinate.

4.1.3 The total wave field

The total wave potential functions in the half-space are

$$\phi_s=\phi^{(r)}+\phi_{s2}+\phi_{s3}\,,\quad \psi_s=\psi^{(i+r)}+\psi_{s2}+\psi_{s3}\qquad(4.16)$$

The total wave potential functions in the saturated soil deposits and water are in the same expressions. In the saturated soil deposits, the potential functions associated with the solid phase

$$\phi_v=\phi_{1,v1}+\phi_{2,v1}+\phi_{1,v2}+\phi_{2,v2}+\phi_{1,v3}+\phi_{2,v3}\,,\quad \psi_v=\psi_{v1}+\psi_{v2}+\psi_{v3}\qquad(4.17)$$

The potential functions associated with the fluid phase

$$\Phi_v=\eta_1[\phi_{1,v1}+\phi_{1,v2}+\phi_{1,v3}]+\eta_2[\phi_{2,v1}+\phi_{2,v2}+\phi_{2,v3}]\,,\quad \Psi_v=\eta_3(\psi_{v1}+\psi_{v2}+\psi_{v3})\qquad(4.18)$$

where η_1, η_2 and η_3 have been defined before.

The potential function in the layer of fluid medium: $\phi_w=\phi_{w2}+\phi_{w3}$ (4.19)

4.2 Solution of the problem

It is seen that the total wave field must satisfy the boundary conditions of the problem, i.e. Eqns. (3.6)-(3.8). The boundary conditions are present in the forms of displacement and stress, so it is important to get the potential-displacement-stress relations firstly.

According to Eqns. (2.2) and Eq. (2.3), these relations of fluid-saturated porous medium for the plane strain problem based on cylindrical coordinates can be obtained as following

$$\left.\begin{aligned}&u_r^v=\frac{\partial\phi_v}{\partial r}+\frac{1}{r}\left(\frac{\partial\psi_v}{\partial\theta}\right),\ u_\theta^v=\frac{1}{r}\frac{\partial\phi_v}{\partial\theta}-\frac{\partial\psi_v}{\partial r},\ U_r^v=\frac{\partial\Phi_v}{\partial r}+\frac{1}{r}\left(\frac{\partial\Psi_v}{\partial\theta}\right),\ U_\theta^v=\frac{1}{r}\frac{\partial\Phi_v}{\partial\theta}-\frac{\partial\Psi_v}{\partial r},\ \sigma=Q\nabla^2\phi_v+R\nabla^2\Phi_v\\&\tau_{rr}^v=A\nabla^2\phi_v+Q\nabla^2\Phi_v+2N\left(\frac{\partial^2\phi_v}{\partial r^2}\right)+2N\left[\frac{\partial}{\partial r}\left(\frac{1}{r}\frac{\partial\psi_v}{\partial\theta}\right)\right],\tau_{r\theta}^s=2N\left(\frac{1}{r}\frac{\partial^2\phi_v}{\partial r\partial\theta}-\frac{1}{r^2}\frac{\partial\phi_v}{\partial\theta}\right)+N\left(\frac{1}{r^2}\frac{\partial^2\psi_v}{\partial\theta^2}-r\frac{\partial}{\partial r}\left(\frac{1}{r}\frac{\partial\psi_v}{\partial r}\right)\right)\end{aligned}\right\}\ (4.20)$$

The relations of single-phase solid medium for the plane strain problem based on cylindrical coordinates were obtained by Pao and Mow [24].

$$\left.\begin{aligned}&\tau_{rr}^s=\lambda\nabla^2\phi_s+2\mu\left[\frac{\partial^2\phi_s}{\partial r^2}+\frac{\partial}{\partial r}\left(\frac{1}{r}\frac{\partial\psi_s}{\partial\theta}\right)\right],\tau_{r\theta}^s=\mu\left[2\left(\frac{1}{r}\frac{\partial^2\phi_s}{\partial r\partial\theta}-\frac{1}{r^2}\frac{\partial\phi_s}{\partial\theta}\right)+\left(\frac{1}{r^2}\frac{\partial^2\psi_s}{\partial\theta^2}-r\frac{\partial}{\partial r}\left(\frac{1}{r}\frac{\partial\psi_s}{\partial r}\right)\right)\right]\\&u_r^s=\frac{\partial\phi_s}{\partial r}+\frac{1}{r}\frac{\partial\psi_s}{\partial\theta},u_\theta^s=\frac{1}{r}\frac{\partial\phi_s}{\partial\theta}-\frac{\partial\psi_s}{\partial r}\end{aligned}\right\}\ (4.21)$$

The relations of the fluid medium can be written as

$$\tau_{rr}^w=K_f\nabla^2\phi_w,\quad u_r^w=\frac{\partial\phi_w}{\partial r}\qquad(4.22)$$

Substituting the potential functions of the total wave field into Eqns. (4.20)-(4.22) and applying the boundary conditions (3.6)- (3.8), a set of equations in terms of the undetermined coefficients in Eqns. (4.8) - (4.14) can be got. It should be pointed out that the above equations are all in infinite sum, therefore, the system of equations must be solved by truncating the infinite terms into finite terms. The number of terms included in the calculation must be large enough to reach the required accuracy and is generally dependent on the input frequency, ω, the radius of the valley, b_2, and the shear wave velocity of the incidence wave. The dimensionless frequency is defined as $\eta = \frac{2b_2}{\lambda_2} = \frac{k_2 a}{\pi}$ (where λ_2 and k_2 are the shear wavelength and wave number of the incident wave, respectively). The number of terms included in the calculation is increase with the value of the dimensionless frequency, η, and is as high as 36 for η=2 to this problem.

5. STUDY ON THE INFLUENCE FACTORS OF THE EARTHQUAKE GROUND MOTIONS OF LOCAL SITES WITH SATURATED SOIL

From the point of view of earthquake engineering and strong motion seismology, an important aspect of above analysis is the description of displacement amplitudes at various points along the surface of the site. Once the wave potential functions have been determined, the displacement vector can be obtained easily. In this paper, the influence factors of the earthquake ground motions of cylindrical canyons in saturated porous medium and circular-arc alluvial valleys with saturated soil deposits are mainly studied.

For cylindrical canyons in saturated porous medium

(1) The complexity of the surface displacement amplitudes, caused by the presence of the circular cylindrical canyon, increases with increasing frequency, η. At low frequencies, the incidence waves have long wavelengths, when compared with the radius of the canyon, a_1, the long waves do not 'feel' the short topographic irregularities. As the frequency increases, the complexity of the surface displacement amplitudes of the solid phase increases on the side of the half space facing the incoming waves(x/a<-1), and becomes relatively smoother on the other side(x/a>1). But either or both of the horizontal and vertical components of displacement on the side of x/a>1 are not smaller, and can even be larger than those in front of the canyon on the side x/a<-1. For incident SV-wave, the horizontal components of displacement on the side of x/a<-1 increase dramatically when incidence beyond critical angle, and the surface displacement amplitudes at the point x/a=-1 seriously fluctuates.

(2) In general, the surface displacement amplitudes under the impervious conditions are larger than that under the pervious conditions.

(3) The relative stiffness of the solid skeleton, μ/K_f, has great influence on the surface displacement. The effects of variations in Poisson's ratio are significant for the solid-dominated case (i.e. large μ/K_f ratio), especially when the frequency is low, and diminish with decreasing solid stiffness. When the μ/K_f is smaller, the surface displacement amplitudes may be very large. Under the same conditions, the amplification of the surface displacements, due to the cylindrical canyons in soft saturated soil(i.e. small μ/K_f ratio), is much larger by assuming the soil as a saturated porous medium than an elastic single-phase elastic medium, especially when the boundary is impervious. So, for soft soil, big error may occur when the soil assumed as elastic single-phase elastic medium.

(4) The cases that the degree of saturation, S_r, is sufficiently high (e.g. higher than 90%) so that the air is embedded in pore water in the form of bubbles [25] are considered in this study. For this special case, the concept of homogeneous pore fluid could be applied to the theory of two-phase porous media as described in Ref. [26]. The result shows that, the surface displacements of the canyons may show evident changes, when the degree of saturation has a very small change compared with the complete saturation. But for the condition of S_r<100%, the degree of saturation has little influence on the surface displacement.

For circular-arc alluvial valleys with saturated soil deposits

(1)The valleys with saturated soil deposits have strong amplifying action to the surface displacements. And the amplification of the surface displacements within the valley, is much larger than that outside the valley. The valleys with saturated soil deposits also have the stronger filtering action. Regarding the fixed location, the filtering action caused by the valleys adds with increasing of the frequency of the incident waves. The surface displacements of valleys depend strongly on the frequency, angle of incidence, and its position.

(2) In general, the amplification of the surface displacements by the presence of the deep alluvial valleys are larger than shallow valleys. But the amplification of the surface displacements by the presence of the shallow alluvial valleys can not be neglected. In some conditions, the surface displacements of a few points in the shallow alluvial valleys may be relatively large.

(3) When the deposits is soft (i.e. the relative stiffness of the solid skeleton of the deposits, μ/K_f, is small), the surface displacement amplitudes may very large and change greatly. But the effects of μ/K_f on the surface displacement amplitudes are very complex, so one can not say that the surface displacement amplitudes

increases with decreasing μ/K_f.
(4) In a wide frequency band, the surface displacement amplitudes under the impervious conditions are larger than that under the pervious conditions. And the range of the frequency band is related to the incident angle.
(5) The amplification of the surface displacements, due to the circular-arc alluvial valleys with the soil deposit being assumed as a saturated porous medium is quite different from that due to the valleys with the soil deposit being assumed as an elastic single-phase elastic medium. And in some case, the amplification of the surface displacements, due to the valleys in saturated soil, is much larger by assuming the soil as a saturated porous medium than an elastic single-phase elastic medium, especially when the boundary is impervious.

6. CONCLUSION

This paper presents a series of analytical solutions for scattering of plane P and SV waves by several typical sites with saturated soil, which include: (1) cylindrical canyons in saturated porous medium; (2) alluvial valleys with saturated soil deposits; (3) circular-arc layered valleys consisting of the interaction between water and saturated soil deposits; (4) cylindrical cavity in a fluid-saturated porous media half space. Based on these solutions, the earthquake ground motions of cylindrical canyons in saturated porous medium and circular-arc alluvial valleys with saturated soil deposits are mainly studied. From the studies, one can find that the ground motions of the saturated soil local irregular site not only depend on the topography of the local site (such as the depth-to-width ratio of canyons or valleys) and the characteristic of the incident waves (i.e. the frequency and the angle of incidence), but also depend on the material characteristic of the soil and the boundary conditions. At the same time, the soft saturated soil site can be simulated by elastic one-phase solid model or by fluid-saturated porous media model, but the results of the ground motion by the two models were great different.

ACKNOWLEDGEMENTS

The study was financially supported by the Natural Science Foundation of P.R. China. (Grant No.50708005).

REFERENCES

[1] Singh,S.K.,Mena,E.,Castro,R. (1988). Some aspects of source characteristics of the 19 September 1985 Michoacan earthquake and ground motion amplification in and near Mexico City from strong motion data. *Bulletin of Seismological Society of America* **78:2**, 451.
[2] Trifunac M D. (1973). Scattering of plane SH wave by a semi-cylindrical canyon. *Int. J. Earthquake Eng. and Struct. Dynamic*: **1**, 267-281.
[3] Trifunac M D. (1971). Surface motion of semi-cylindrical alluvial valley for incident plane SH waves. *Bulletin of Seismological Society of America*: **61**, 1755-1770.
[4] Wong H L and Trifunac M D. (1974a). Scattering of plane SH-wave by a semi-elliptical canyon. *Soil Dynamics and Earthquake Engineering* **9:3**, 157-169.
[5] Wong H L and Trifunac M D. (1974b). Surface motion of semi-elliptical alluvial valley for incident plane SH waves. *Bulletin of Seismological Society of America* **64:1**, 1389-1408.
[6] Cao H and Lee V W. (1990). Scattering and diffraction of plane P waves by circular-cylindrical canyons with variable depth-to-width ratio. *Soil Dynamics and Earthquake Engineering* **9:3**, 141-150.
[7] Lee V W and Cao H. (1989). Diffraction of SV by circular canyons of various depth. *Journal of Engineering Mechanics, ASCE* **115:9**, 2035-2056.
[8] Todorovska M and Lee V W. (1991). Surface motion of shallow circular alluvial valleys for incident plane SH waves: analytical solution. Soil Dynamics and Earthquake Engineering. **4**,192-200.
[9] Yuan X and Liao Z. (1995). Scattering of plane SH wave by a cylindrical alluvial valley of circular-arc cross-section. *Earthquake engineering and Structure Dynamics* **24:1**, 1303-1313.
[10] Liang Jianwen, Yan Linjun, and et.al. (2001). Response of circular-arc alluvial valleys under incident plane P waves. *Rock and Soil Mechanics (in Chinese)* **22:2**, 138-143.
[11] Liang Jianwen, Yan Linjun, Lee V W. (2001). Scattering of plane P waves by circular-arc layered alluvial valleys: an analytical solution. *Acta Seismologica Sinica (in Chinese)* **23:2**, 167-184.
[12] Lee V W. (1984). Three dimensional diffraction plane P, SV and SH wave by a hemisherical alluvial valley. *Soil*

Dynamics and Earthquake Engineering **3:3**, 133-144.
[13] Lee V W. (1982). Note on the scattering of elastic plane waves by a hemisherical alluvial valley. *Soil Dynamics and Earthquake Engineering* **1:3**, 122-129.
[14] Li Weihua. (2004). Analytical Solutions and Numerical Simulation of the Scattering Plane Waves by Local Sites with Saturated Soil (Doctoral Dissertation). Beijing: Beijing Jiaotong University. P. R. China.
[15] Zhao Chenggang, Du Xiuli, and et.al.. (1998). Review of wave propagation theory in saturated and unsaturated porous medium and its numerical methods. *Advances in Mechanics (in Chinese)* **28:1**, 83-92
[16] Biot M A. (1956). Theory of propagation of elastic wave in fluid-saturated porous soil. *The Journal of the Acoustical Society of America*. **28**(2): 168-178
[17] Xu Changjie, Wu Shiming. (1998). Spherical wave propagation in saturated soils. Applied Mathematics and Mechanics **19:3**, 223-230.
[18] Hu Ya-yuan, Wang Li-zhong, Chen yun-min, et al. (1998). Scattering and refracting of plane strain wave by a cylindrical inclusion in fluidsaturated soils. *Acta Seismologica Sinica (in Chinese)* **20(3)**: 300-307.
[19] Deresiewicz H and Rice J T. (1962). The effect of boundaries wave propagation in a liquid-filled porous solid: □. Reflection of plane waves at a free plane boundary (general case). *Bulletin of Seismological Society of America* **52:3**, 595-625.
[20] Deresiewicz H, et al. (1963). On uniqueness in dynamic poro-elasticity. *Bulletin of Seismological Society of America* **53**:595-626.
[21] Hajra S, et al. (1982). Reflection and refraction of seismic waves incident obliquely at the boundary of a liquid-saturated porous solid. *Bulletin of Seismological Society of America* **72**:1509-1533.
[22] Wang Weijia. (1984). The wave in the viscous compressible fluid. *Chinese Journal of Geophysics (in Chinese)* **27:1**, 84~93
[23] Watson GN. (1962). A Treatise on the Theory of Bessel Functions. Cambridge, Cambridge University Press.
[24] Pao Y H, Mow C C. (1973). The Diffraction of Elastic Waves and Dynamic Stress Concentrations. New York : Crane & Russak.
[25] Verruijt A. (1969). Elastic Storage Aquifers. Flow Through Porous Media .London: Academic Press.
[26] Chang CS, et al. (1983). Consolidation analysis for partly saturated clay by using an elastic–plastic effective stress–strain mode. *Int J Numer Anal Meth Geomech* **7**:39–56.